Cronfa - Swansea University Open Access Repository

_____

This is an author produced version of a paper published in :
Journal of Alloys and Compounds

_____

Cronfa URL for this paper:

_____

Paper:

_____

Meso-microstructural computational simulation of the hydrogen permeation test to calculate intergranular, grain boundary and effective diffusivities.

S.Jothi[*a], N. Winzer[b], T.N.Croft[a], S.G.R.Brown[a]

[a] College of Engineering, Swansea University, Singleton Park, Swansea SA2 8PP, UK

[b] Fraunhofer Institute for Mechanics of Materials IWM, Wöhlerstraße 11, 79108 Freiburg, Germany

E-mail: *s.jothi@swansea.ac.uk

ABSTRACT:

Hydrogen induced intergranular embrittlement has been identified as a cause of failure of aerospace components such as combustion chambers made from electrodeposited polycrystalline nickel. Accurate computational analysis of this process requires knowledge of the differential in hydrogen transport in the intergranular and intragranular regions. The effective diffusion coefficient of hydrogen may be measured experimentally, though experimental measurement of the intergranular grain boundary diffusion coefficient of hydrogen requires significant effort. Therefore an approach to calculate the intergranular GB hydrogen diffusivity using finite element analysis was developed. The effective diffusivity of hydrogen in polycrystalline nickel was measured using electrochemical permeation tests. Data from electron backscatter diffraction measurements were used to construct microstructural representative volume elements including details of grain size and shape and volume fraction of grains and grain boundaries. A Python optimization code has been developed for the ABAQUS environment to calculate the unknown grain boundary diffusivity.

Keywords: Computer simulations, hydrogen absorbing materials, diffusion, grain boundaries, microstructure, mechanical properties.

1. Introduction

Grain boundary (GB) diffusion plays an important role in many processes occurring in engineering materials [1-5, 16-18], including intergranular cracking due to hydrogen embrittlement (HE) [4-8]. Reliable information on GB diffusion properties can be used in the development and processing of new and existing metals and alloys in order to reduce their susceptibility to cracking and failure [2, 6, 9-10, 15-18]. Traditionally grain boundary diffusion may be characterised experimentally using radioactive tracers, secondary ion mass

spectroscopy (SIMS) or by using bi-crystal electrochemical permeation tests. These techniques are expensive, time consuming, challenging to perform and only provide data for one specific grain boundary orientation [9-12]. Van Loo also noted that small experimental errors can result in significant errors in the measurement of GB diffusivity [11-12]. It would therefore be useful to develop the ability to estimate GB diffusivity using computational techniques that could also allow the accuracy of experimental diffusion measurements to be assessed. This paper presents a microstructure-based multi-scale finite element (FE) computational approach that uses experimentally-collected electron backscatter diffraction (EBSD) data to calculate the GB diffusivity of hydrogen in polycrystalline nickel.

2. Experimental procedures

2.1 Material

The material used in this study was electrodeposited polycrystalline pure nickels in the form of 75 μm thick thin foil with 3 μm average grain size.

2.2 Electrochemical permeation test

The experimental electrochemical permeation test was carried out according to ISO 17081 using a cell divided into two chambers, "cathodic" (i.e. charging chamber) and "anodic" (i.e. detection chamber), separated by the sample nickel foil. The electrolyte used in the cathodic chamber was 0.5M H_2SO_4 whereas that used in the anodic chamber was 0.1M NaOH. A detailed description of the experimental process can be found elsewhere [13]. The effective diffusion coefficient is calculated from the measured permeation curves according to Equation 1.

$$D_{eff} = L^2/(6\,t_L) \tag{1}$$

Where, L is the thickness of the specimen and t_L is the so-called lag time (the time required for the hydrogen flux through the sample surface in the detection chamber to reach 0.63 of its steady state current). Under steady state conditions the sub-surface concentration of hydrogen at the entry side (C_{entry}) in the charging chamber was calculated according to Equation 2.

$$C_{entry} = \frac{I_{max}\,L}{A\,E_c\,D_{eff}} \tag{2}$$

In the above equations I_{max} is the steady-state permeation current density, A is the area of the sample and E_c is the elementary charge.

2.3 EBSD analysis

EBSD analysis was performed on the nickel foils after permeation tests had been conducted. Initially, samples were prepared for EBSD analysis by grinding the surface with up-to 600 grade SiC paper and then polishing with 9, 3 and 1 μm diamond paste and, finally, with 0.05 μm colloidal silica for 30 minutes. Crystal orientation maps and data were obtained using Oxford Instruments HKL Technology Channel 5 EBSD system integrated with a Philips XL30 scanning electron microscope (SEM) operating at 20 kV using a 0.1 μm step size. The orientation data was post processed to remove spurious observations using the grain dilatational clean up module in the HKL software (square grid mapping) and converted to TSL (TexSEM Laboratories Ltd) orientation image mapping (OIM) software (hexagonal grid format) by collecting the required GB dataset. The collected GB dataset was reconstructed, processed and displayed using EDAX TSL OIM software.
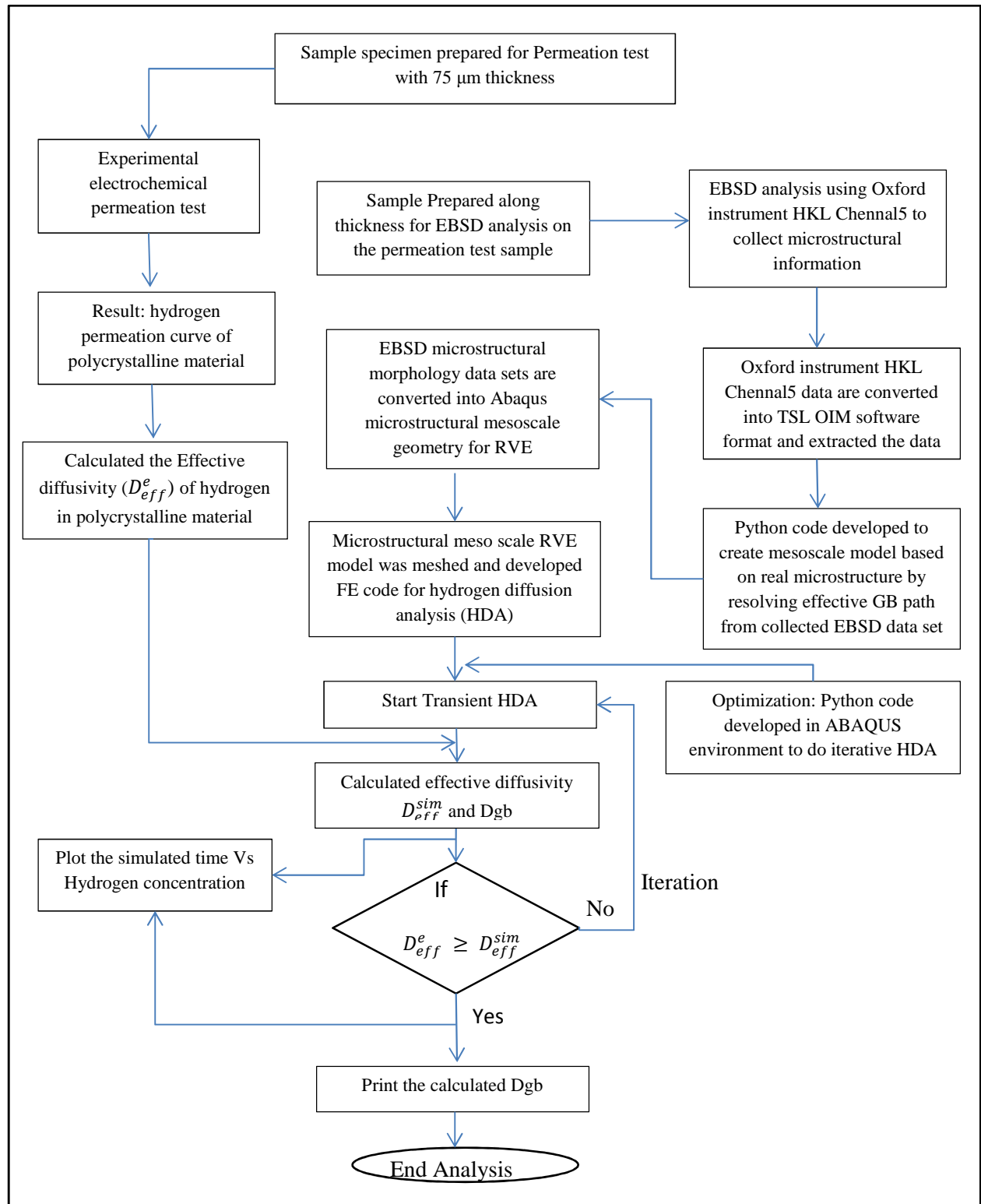
3. Computational modelling approach:

In this work the real microstructure has been extracted from EBSD analysis data. An algorithm was developed to extract data from EBSD data files and convert them into Abaqus mesoscale microstructural meshes. The Abaqus geometric model uses the following information extracted from the EBSD data:

- Grain shape, size and structure of the observed microstructure.
- Volume fractions of grains, grain boundaries and triple junctions.
- Statistical distributions of the crystal orientation and grain boundary misorientations.

In the computational model the grain boundaries were assigned a thickness of 10 Å [6] to form "grain boundary affected zones" (GBAZ). This allows the enhanced diffusivity associated with the grain boundaries to be accounted for numerically. A mesh sensitivity analysis was performed to determine suitable meshes in the grains and GBAZs. In the microstructural FE model [14] the hydrogen enters into the material from one side of the computational grid. It is assumed that there is no hydrogen initially present in the material. The effective hydrogen diffusivity along grain boundaries (D_{gb}) (i.e the effective grain boundary diffusivity are incorporated with types of grain boundaries diffusivities with in the current model) was initially assumed to be equal to the standard lattice diffusivity (D_g=3.52×10^{-10} cm^2/s) [6]. This was then increased in increments of 2×10^{-9} cm^2/s until the

overall diffusivity corresponds to that obtained from the permeation test. The detail computational approach is shown in the flowchart1.

```
┌─────────────────────────────────────────────────────────────────────────────┐
│                                                                               │
│              Sample specimen prepared for Permeation test                     │
│                        with 75 μm thickness                                   │
│                                                                               │
│   ┌──────────────┐        ┌──────────────┐          ┌──────────────┐          │
│   │ Experimental │        │ Sample       │          │ EBSD analysis│          │
│   │ electrochem- │        │ Prepared     │          │ using Oxford │          │
│   │ ical         │        │ along        │          │ instrument   │          │
│   │ permeation   │        │ thickness for│          │ HKL Chennal5 │          │
│   │ test         │        │ EBSD analysis│          │ to collect   │          │
│   │              │        │ on the       │          │ microstruct- │          │
│   │              │        │ permeation   │          │ ural         │          │
│   │              │        │ test sample  │          │ information  │          │
│   └──────────────┘        └──────────────┘          └──────────────┘          │
└─────────────────────────────────────────────────────────────────────────────┘
```

Sample specimen prepared for Permeation test with 75 μm thickness

Experimental electrochemical permeation test

Sample Prepared along thickness for EBSD analysis on the permeation test sample

EBSD analysis using Oxford instrument HKL Chennal5 to collect microstructural information

Result: hydrogen permeation curve of polycrystalline material

EBSD microstructural morphology data sets are converted into Abaqus microstructural mesoscale geometry for RVE

Oxford instrument HKL Chennal5 data are converted into TSL OIM software format and extracted the data

Calculated the Effective diffusivity (D_{eff}^e) of hydrogen in polycrystalline material

Microstructural meso scale RVE model was meshed and developed FE code for hydrogen diffusion analysis (HDA)

Python code developed to create mesoscale model based on real microstructure by resolving effective GB path from collected EBSD data set

Start Transient HDA

Optimization: Python code developed in ABAQUS environment to do iterative HDA

Calculated effective diffusivity D_{eff}^{sim} and Dgb

Plot the simulated time Vs Hydrogen concentration

Iteration

If

$D_{eff}^e \geq D_{eff}^{sim}$

No

Yes

Print the calculated Dgb

End Analysis

Flowchart1: Flowchart shows the detail about the computational approach developed in this study to calculate the effective GB diffusivity of hydrogen in polycrystalline nickel.

4. Results and discussions

4.1. Experimental electrochemical permeation test result:

Electrochemical permeation tests have been performed on 75μm thick polycrystalline nickel sample foil with and the resulting current density as a function of time has been analysed using the equation (1), (2) and (3) to calculate the effective diffusivity of bulk polycrystalline nickel. The experimentally-determined effective hydrogen diffusivity (D_{eff}^e) was calculated using Equation 1 to be 4.1327×10^{-10} cm^2/s [13].
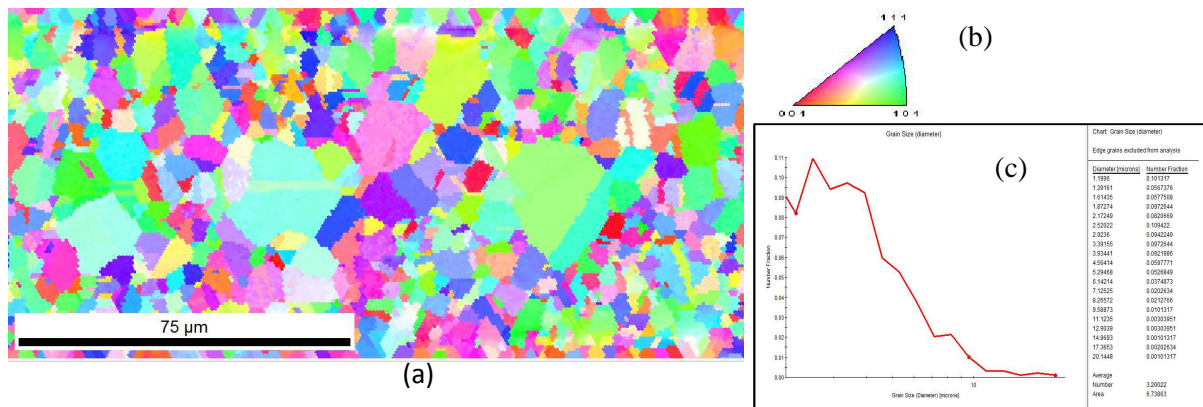
Figure1: (a) EBSD analysis results for the cross-section of the nickel foil (b) inverse pole figure, (c) grain size distribution.
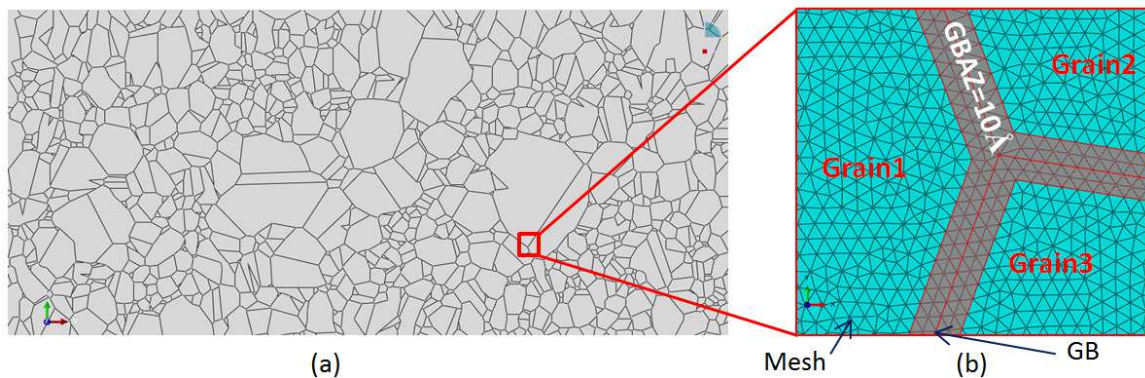
Figure2: (a) Abaqus FE meso scale microstructural model based on the EBSD data shown in Figure 1 (b) detail of the FE mesh near triple junction of the three neighbouring grains showing the GBAZ (red region) with a thickness of 10Å.

4.2. Experimental EBSD analysis results:

EBSD orientation mapping was done on the cross-section of the nickel foil used for electrochemical permeation test to determine several metallurgical parameters. The microstructural geometric features were extracted to develop a meso-microstructural RVE for subsequent simulation. The crystallographic orientations within cross section of the nickel foil are shown in Figure 1(a). Figure 1(b) shows the inverse pole figure of the

crystallographic orientation map. The grain diameter distribution is shown in Figure 1(c). The majority of grains have diameters between 1 and 4 μm. The total length of the GB was calculated to be 12015.2 μm.

4.3. Meso scale microstructural computational FE results:

The EBSD data was then used to create a meso-scale microstructural RVE, which was used in FE simulations to determine the theoretical effective diffusivity, D_{eff}^{sim} [4,13]. The RVE model is shown in Figure 2(a). Figure 2(b) shows a magnified view of the FE model near a triple junction with three neighbouring grains, GBs and GBAZs. In the initial FE simulation, it was assumed that $D_{gb}=D_g$. D_{eff}^{sim} was calculated from the theoretical plot of the hydrogen flux versus time. D_{gb} was then systematically increased and the simulation repeated until D_{eff}^{e} and D_{eff}^{sim} converged. A total to 12 iterations were needed for the results to converge. In final solution D_{gb} was equal to 2.2×10^{-8} cm^2/s, which is two orders of magnitude higher than the standard lattice diffusivity. The hydrogen concentration as function of time curve has been plotted and shown in figure3 (a) and figure3 (b) show the close view of it. The results are plotted in Figure 4 and show good agreement with the result published by Tsuru and Latanision [6].
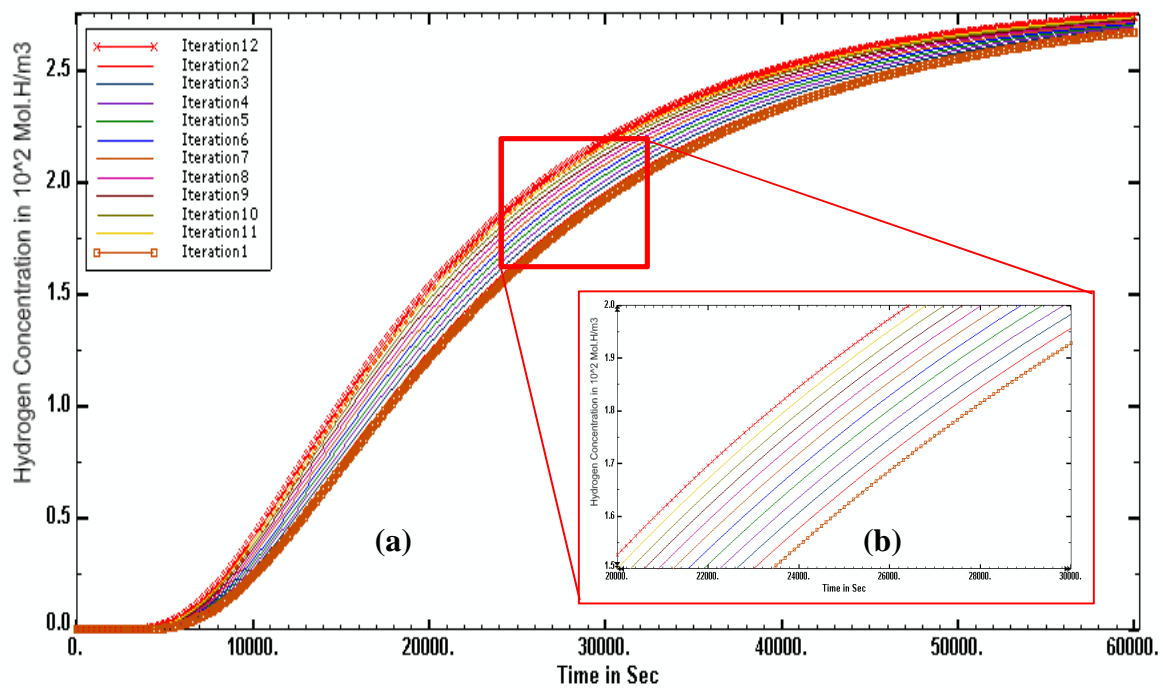

Figure3: Shows the Abaqus mesoscale microstructural polycrystalline nickel FE Simulated results of transient hydrogen diffusion analysis for various iterations. (b) Shows the close view of it.
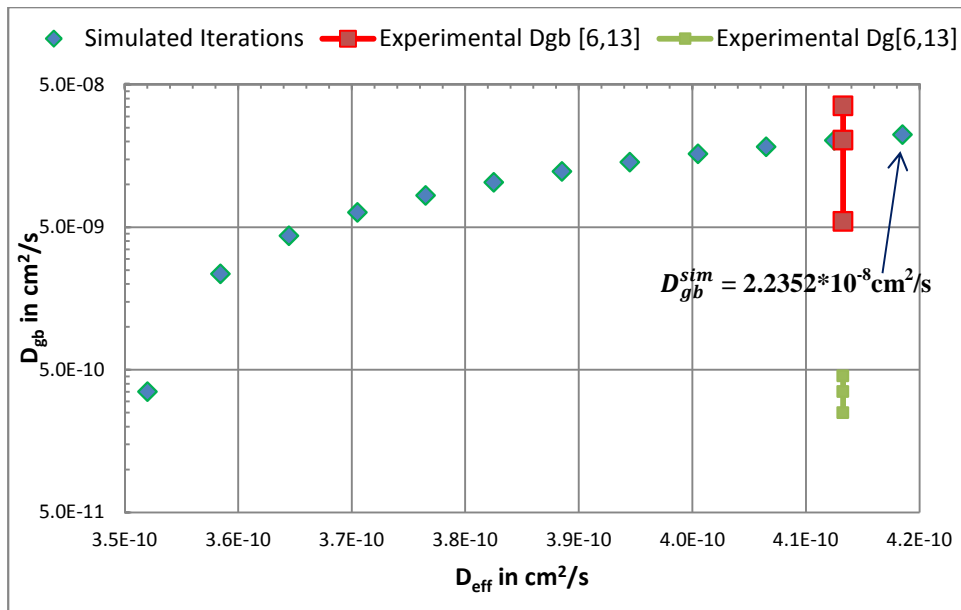
Figure4: Results of the Abaqus meso-microstructural FE simulations for effective grain boundary diffusivity and effective bulk diffusivity for polycrystalline nickel over 12 iterations and experimentally measured results of D_{gb}, lattice diffusivity or grain diffusivity (D_g) from literature [6] and experimentally calculated effective diffusivity from electrochemical permeation tests [13].

5. Conclusion

A meso-scale microstructural FE computational technique has been developed to calculate the diffusivity of hydrogen along grain boundaries in a polycrystalline material. The microstructural model is based on features such as grain size and shape, grain orientations and grain boundary volume fractions extracted from EBSD data. The predicted grain boundary diffusivity is two orders of magnitude higher than the lattice diffusion of hydrogen in nickel. The model results are in good agreement with experimental measurements. Understanding the intergranular diffusion of impurity atoms aids understanding, control and solution of engineering problem such as hydrogen embrittlement. This method could also be used to design new polycrystalline materials with improved resistance to material degradation and failure. The effective grain boundary and its diffusivity are incorporated with types of grain boundaries and its diffusivities with in the current model. This treatment of type of grain boundaries are the limitation of this model. The next step will take into consideration of different types of grain boundaries in the model.

Acknowledgements

References:

[1]   C. Herzig, S.V. Divinski, Grain boundary diffusion in metals: Recent development, Materials Transactions 44 (2003) pp. 14-27.

[2]   S. Jothi, T.N. Croft, S.G.R. Brown, Influence of grain boundary misorientation on hydrogen embrittlement in bi-crystal nickel, International journal of hydrogen energy 39 (2014) pp. 20671-20688.

[3]   I. Kaur, Y. Mishin, W. Gust, Fundamentals of grain and interphase boundary diffusion, Wiley, Chichester, UK (1995).

[4]   S. Jothi, T.N. Croft, S.G.R. Brown, E. de Souza Neto, Finite element microstructural homogenization techniques and intergranular, intragranular microstructure effects on effective diffusion coefficient oh heterogeneous polycrystalline composite media, Composites Structures 108 (2014) pp. 555-564.

[5]   K.A. Esakul, Ed., Handbook of case histories in Failure Analysis, ASM international 1 (1992).

[6]   T. Tsuru, R.M. Latanision, Grain boundary transport of hydrogen in nickel, Scripta Metall 16 (1982) pp. 575-578.

[7]   M.L. Martin, B.P. Somerday, R.O. Ritchie, P. Sofronis, I.M. Robertson, Hydrogen-induced intergranular failure in nickel revisited, Acta Materialia 60 (2012) pp. 2739-2745.

[8]   R.M. Latanision, H. Opperhauser. Jr, Further observations on the effect of grain boundary segregation in the hydrogen embrittlement of nickel, Metallurgical Transactions A 6A (1975) pp. 233-234.

[9]   I.V. Belova, N.S. Kulkarni, Y.H. Sohn and G.E. Murch, Simultaneous measurement of tracer and interdiffusion coefficients: An isotopic phenomenological diffusion formalism for the binary alloy, Philosophical Magazine 93:26 (2013) pp. 3515-3526.

[10]   S. Brennan, K. Bermudez, N.S. Kulkarani, Y. Sohn, Interdiffusion in the MG-Al System and intrinsic diffusion in β-Mg_2Al_3, Metallurgical and Materials Transactions A 43 (2012) pp. 4043-4052.

[11]   F.J.J. van Loo, Multiphase diffusion in binary and ternary solid-state systems, progress in solid state chemistry 20 (1990) pp. 47-99.

[12]   N.S. Kulkarni, C.V. Iswaran, R.T. DeHoff, Intrinsic diffusion simulation for single-phase, multicomponent systems, Acta Materialia 53 (2005) pp. 4097-4110.

[13]   S. Jothi, T.N. Croft, S.G.R. Brown, "EU FP7 Multiscale modelling hydrogen Embrittlement- MultiHy" deliverable 6.2, Swansea University report (2014).

[14]   S. Jothi, T.N. Croft, S.G.R. Brown, E. de Souza Neto, Computational analysis of hydrogen diffusion in polycrystalline nickel and anisotropic polygonal micro, nano grain size effects, International conference on hydrogen safety proceeding, (2013) Belgium.

[15]   S. Brennan, A.P. Warren, K.R. Coffey, N. Kulkarni, P. Todd, M. Kilmov, Y. Sohn, Aluminium impurity diffusion in magnesium, Journal of Phase Equilibria and Diffusion 33 (2012) pp. 121-125.

[16]   A.Oudriss, J. Creus, J. Bouhattate, E. Conforto, C. Berziou,C. Savall, X. Feaugas, Grain size and grain boundary effects on diffusion and trapping of hydrogen in pure nickel, Acta Materialia 60 (2012) 6814-6828.

[17]   S. Jothi, T.N. Croft, S.G.R. Brown, Coupled macroscale-microscale model for hydrogen embrittlement in polycrystalline materials, (In press) (2014) DOI: 10.1016/j.ijhydene.2014.12.068.

[18]   S. Jothi, T.N. Croft, S.G.R. Brown, Multiscale multiphysics model for hydrogen embrittlement in polycrystalline nickel, (In press) (2014) DOI: 10.1016/j.jallcom.2014.12.073.